

Quantum antiferromagnetism in the $d = 3$ Hubbard model — a spin-fluctuation approach

Avinash Singh*

Theoretische Physik III, Elektronische Korrelationen und Magnetismus, Universität Augsburg, D-86135 Augsburg, Germany

A self-consistent spin-fluctuation theory is developed to obtain T_N vs. U for the half-filled Hubbard model in the whole U/t range. Good agreement is obtained in the strong coupling limit with the high-temperature series-expansion result for the equivalent Heisenberg model. Quantum spin-fluctuation correction to the sublattice magnetization is also obtained for all U at the one-loop level. A spin picture is used throughout, and quantum effects are incorporated through transverse spin fluctuations, which are evaluated in the random phase approximation using a new method.

75.10.Jm, 75.10.Lp, 75.30.Ds, 75.10.Hk

Finite-temperature antiferromagnetism within the three-dimensional Hubbard model at half filling involves two fundamentally different aspects. One is the local symmetry breaking at temperatures much smaller than the AF gap parameter Δ , and formation of the local-moment which grows rapidly and saturates with increasing U/t . The other is the scale of low-energy spin excitations, which initially rises along with the charge gap for small U , and then crosses over to an approximately t^2/U fall-off for large U , becoming degenerate, in the strong coupling limit, with the exchange energy scale $J = 4t^2/U$ of nearest-neighbor (NN) spin couplings in the equivalent $S = 1/2$ quantum Heisenberg model. Thus, while in the weak-coupling limit ($U \ll B = 12t$, the free-particle band-width) it is essentially the process of *moment melting* which determines the magnetic transition temperature $T_N \sim \Delta$, in the strong coupling limit ($U \gg B$) it is the *spin disordering* tendency of thermal fluctuations which determines the transition temperature $T_N \sim J$ at which long-range AF order is destroyed. A proper description of the magnetic transition in the whole U/t range within a *single* theory is therefore quite challenging.

Earlier studies of finite-temperature antiferromagnetism within the three-dimensional Hubbard model, aimed at determining T_N vs. U in the whole U/t range, have employed the functional integral formalism, mainly within the static approximation, [1–6] quantum Monte Carlo methods, [7,8] and recently the dynamical mean-field theory, [9] which becomes exact in the limit of infinite dimensions. [10] All share the common feature of yielding a T_N which approaches, in the strong coupling limit, the mean-field-theory (MFT) result for the equivalent spin-1/2 Heisenberg model, $T_N^{\text{MF}} = zt^2/U$, where $z = 2d$ is the lattice coordination number. [11] While this is natural for the functional-integral schemes employing static approximation and the dynamical mean-field theory, due to neglect of the Goldstone mode, high-temperature series expansions yield a substantially lower $T_N \approx 3.83t^2/U$. [3,4,7,8] A recent mean-field approach utilizing the Onsager reaction-field correction yields a T_N

in close agreement. [12] Here account is made of the low-energy spin excitations through an approximate mapping to an effective $S = 1/2$ Heisenberg model with U -dependent, extended-range spin couplings.

In this paper we have considered a spin picture throughout for the description of quantum antiferromagnetism in the Hubbard model. We imagine quantum spins on each site, and incorporate (quantum) transverse spin fluctuations about the (classical) HF state, having local moment $\langle S_z \rangle_{\text{HF}}$. Within this conceptually simple framework we have obtained both the Néel temperature T_N vs. U and the sublattice magnetization m vs. U (at $T = 0$) in the whole U/t range. Transverse spin fluctuations are obtained within the random phase approximation (RPA) in terms of magnon mode energies and amplitudes. A new method is described for evaluating the transverse spin correlations for arbitrary U/t .

As $\langle S_z \rangle_{\text{HF}}$ is the maximum (classical) spin polarization in the z-direction, and therefore also the maximum eigenvalue of the local S_z operator, hence $S \equiv \langle S_z \rangle_{\text{HF}}$ plays the role of the effective spin quantum number. At $T = 0$, quantum corrections to the sublattice magnetization are then obtained at the one-loop level from the RPA-level transverse spin fluctuations. On the other hand, at finite temperature a self-consistent theory is used in which the magnon spectral functions and energies are self-consistently renormalized. Consistent with our RPA-level description in which details beyond this level are ignored, only momentum-independent multiplicative renormalizations are considered. While assumption is made here regarding their form, these renormalizations are basic requirements following from the commutation relations of quantum spin operators, and are further discussed later.

As all calculations are done with RPA-level magnon energies and spectral functions, this provides a RPA-level description of the magnetic phase diagram. Features such as continuous spin-rotational symmetry and transverse spin fluctuations are included, resulting in substantial improvement over the HF theory. Proper limiting results are therefore obtained as $d \rightarrow 2$ ($T_N \rightarrow 0$, for all U), and

$d \rightarrow \infty$ ($T_N \rightarrow T_N^{\text{MF}}$, for $U/t \rightarrow \infty$).

We first discuss the approach for determining the Néel temperature within the spin picture used here in terms of the local spin operators \vec{S}_i . In the anisotropic broken-symmetry state for $T < T_N$, we have $\langle S_i^z S_i^z \rangle > \langle \vec{S}_i^2 \rangle / 3$. However, with increasing temperature the anisotropy progressively decreases, and eventually vanishes at the Néel temperature. Therefore we determine T_N from the following isotropy requirement,

$$\langle S_i^- S_i^+ \rangle = \langle S_i^+ S_i^- \rangle = (2/3) \langle \vec{S}_i^2 \rangle \quad \text{as } T \rightarrow T_N^-. \quad (1)$$

I. STRONG COUPLING LIMIT

We self consistently obtain the enhancement in transverse spin fluctuation $\langle S_i^- S_i^+ \rangle$ due to thermal excitation of magnons. The amplitude of the magnon propagator and the magnon energy are both multiplicatively renormalized by $\langle S^z \rangle$, the sublattice magnetization. This follows from a finite-temperature extension of the one-loop correction to the magnon propagator, obtained earlier in the strong correlation limit. [13] Alternatively, in the equivalent spin- S Heisenberg model, this can be seen within the equation of motion approach, [14] which has been applied recently to the $S = 1/2$ case of layered antiferromagnets. [15] Considering first the simpler case of strong coupling, we therefore have for the transverse spin fluctuation,

$$\langle S_i^- S_i^+ \rangle = \langle 2S^z \rangle \sum_q \left[\frac{1}{\sqrt{1-\gamma_q^2}} \frac{1}{e^{\beta\omega_q} - 1} + \frac{1}{2} \left(\frac{1}{\sqrt{1-\gamma_q^2}} - 1 \right) \right], \quad (2)$$

where $\beta = 1/T$ with k_B set to 1, the magnon energy $\omega_q = zJ\langle S^z \rangle \sqrt{1-\gamma_q^2}$, and the two terms are respectively the thermal and quantum (zero-point) contributions. $\langle S_i^+ S_i^- \rangle$ is given by a similar equation except with $[(1-\gamma_q^2)^{-1/2} + 1]$ for the quantum contribution. The renormalization of the magnon propagator by the magnitude $\langle 2S^z \rangle$ in Eq. (2) ensures that the commutation property of spin angular momentum operators $[S^+, S^-] = 2S^z$ is obeyed by the expectation value in the spin state. As $\langle S^z \rangle$ vanishes in the limit $T \rightarrow T_N^-$, from the isotropy requirement we obtain the Néel temperature,

$$T_N = zJ \frac{S(S+1)}{3} f_{\text{SF}}^{-1}, \quad (3)$$

where the spin-fluctuation correction factor $f_{\text{SF}} \equiv \sum_q 1/(1-\gamma_q^2)$ in terms of $\gamma_q = \sum_{\mu=1}^d \cos q_\mu/d$. For the simple cubic lattice $f_{\text{SF}} = 1.517$. As the mean-field result is $T_N^{\text{MF}} = zJS(S+1)/3$, for the spin- S Heisenberg model, spin fluctuations reduce T_N to nearly 70% of its MF value.

For $S = 1/2$ this yields $T_N = 3.95t^2/U$, in good agreement with the result $3.83t^2/U$ from high-temperature series expansions. [16] Furthermore, as the Goldstone mode is built-in, the spin fluctuation theory also yields the appropriate T^2 -falloff of the sublattice magnetization at low temperatures ($T \ll T_N$), and the vanishing of T_N in two dimensions, where f_{SF} diverges.

Interestingly, for hypercubic lattices this spin-fluctuation correction exactly matches with the Onsager-correction to the mean-field result. [17] Here one obtains the reaction-field correction factor $f_{\text{ORF}} = \sum_q 1/(1+\gamma_q)$, which is identically equal to the spin-fluctuation correction factor f_{SF} for hypercubic lattices. It is thus quite a coincidence that while the (Onsager-corrected) MFT and SFT yield very different falloff of staggered magnetization with temperature, identical Néel temperature is obtained in both theories for all S .

The Onsager correction has recently been utilized to discuss the finite-temperature magnetism in the Hubbard model. [12] Here the low-energy excitations of the Hubbard model are approximately mapped to those of an effective $S = 1/2$ Heisenberg model with U -dependent, extended-range spin couplings. The subsequent use of mean field theory, however, does not properly account for the continuous spin-rotational symmetry of the system, resulting in an expression for T_N which is insensitive to whether the effective spin model is of the Heisenberg or Ising type. As a vanishing Néel temperature would be obtained even for the Ising AF on a square lattice, the divergence of the reaction-field correction in two dimensions should therefore be seen as a breakdown of the ORF theory in two dimensions, rather than a source of the vanishing of T_N . Consideration of the gapless spin-fluctuation modes is essential for this.

II. GENERAL CASE

A. Evaluation of transverse spin fluctuations ($T = 0$)

In order to extend these results to arbitrary U/t , we need the magnon mode energies and spectral functions, and we now describe a new method for evaluating transverse spin fluctuations at the RPA level, from which both the Néel temperature and the quantum spin-fluctuation correction to sublattice magnetization are obtained. In addition to the pure antiferromagnets in two and three dimensions, this approach is applicable to a variety of other systems such as AF with disorder, defects, vacancies etc., and provides a simple way to obtain first-order spin-fluctuation corrections about the HF-level broken-symmetry state. The method is based on a convenient way to perform the frequency integral to obtain spin correlations from spin propagators, and we illustrate it here for transverse spin correlations. We write the time-ordered transverse spin propagator

$\langle \Psi_G | T[S_i^-(t)S_j^+(t')] | \Psi_G \rangle$ at the RPA level in frequency space as,

$$\chi^{-+}(\omega) = \frac{\chi^0(\omega)}{1 - U\chi^0(\omega)} = \sum_n \frac{\lambda_n(\omega)}{1 - U\lambda_n(\omega)} |\phi_n(\omega)\rangle \langle \phi_n(\omega)|, \quad (4)$$

where $\phi_n(\omega), \lambda_n(\omega)$ are the eigensolutions of the $\chi^0(\omega)$ matrix. Here $\chi^0(\omega)$ is the zeroth-order, antiparallel-spin particle-hole propagator, evaluated in a suitable basis in the self-consistent, broken-symmetry state at the HF level. In the site representation for instance, $[\chi^0(\omega)]_{ij} = i \int (d\omega'/2\pi) G_{ij}^\dagger(\omega') G_{ji}^l(\omega' - \omega)$ in terms of the HF-level Green's functions. Spin correlations are then obtained from,

$$\begin{aligned} \langle S_i^-(t)S_j^+(t') \rangle &= -i \int \frac{d\omega}{2\pi} [\chi^{-+}(\omega)]_{ij} e^{-i\omega(t-t')} \\ &= \pm \sum_n \frac{\phi_n^i(\omega_n)\phi_n^j(\omega_n)}{U^2(d\lambda_n/d\omega)_{\omega_n}} e^{-i\omega(t-t')}, \end{aligned} \quad (5)$$

where the collective mode energies ω_n are obtained from $1 - U\lambda_n(\omega_n) = 0$, and $\lambda_n(\omega)$ has been Taylor-expanded as $\lambda_n(\omega) \approx \lambda_n(\omega_n) + (\omega - \omega_n)(d\lambda_n/d\omega)_{\omega_n}$ near the mode energies to obtain the residues. For convergence, the retarded (advanced) part of the time-ordered propagator χ^{-+} , having pole below (above) the real- ω axis, is to be taken for $t' < t$ ($t' > t$). The frequency integral is conveniently replaced by an appropriate contour integral in the lower or upper half-plane in the complex- ω space for these two cases, respectively, which results in Eq. (5).

For the pure AF case, it is convenient to use the two-sublattice representation due to translational symmetry, and we work with the 2×2 matrix $[\chi^0(q\omega)]$, which is given in terms of eigensolutions of the HF Hamiltonian, [18] and numerically evaluated using a momentum grid with $\Delta k = 0.1$. Equal-time, same-site transverse spin correlations are then obtained from Eq. (5) by summing over the different q modes. We consider $t' \rightarrow t^-$, so that the retarded part is used, with positive mode energies. From spin-sublattice symmetry, correlations on A and B sublattice sites are related via $\langle S^+S^- \rangle_A = \langle S^-S^+ \rangle_B$.

B. Quantum correction to sublattice magnetization

From the commutation relation $[S^+, S^-] = 2S^z$, the difference $\langle S^+S^- - S^-S^+ \rangle_{\text{RPA}}$ should yield $\langle 2S^z \rangle_{\text{HF}}$, which is indeed confirmed as shown in Fig. 1. The deviation at small U is presumably because of the finite grid size used in the calculations. The sum $\langle S^+S^- + S^-S^+ \rangle_{\text{RPA}}$ yields a measure of transverse spin fluctuations about the HF state, and for spin S in the strong coupling limit, one obtains $\langle S^+S^- + S^-S^+ \rangle_{\text{RPA}} = (2S) \sum_q 1/\sqrt{1 - \gamma_q^2}$. [13,19] Using the identity, $\langle S^z S^z \rangle = S(S+1) - \langle S^+S^- + S^-S^+ \rangle/2$, the sublattice magnetization $m = \langle 2S^z \rangle$ is then obtained from, [20]

$$\langle S^z \rangle = S \left[1 - \frac{1}{S} \left(\frac{\langle S^+S^- \rangle + \langle S^-S^+ \rangle}{2S} - 1 \right) \right]^{1/2}. \quad (6)$$

To order $1/2S$, this yields the correction to the sublattice magnetization of $(2S)^{-1} \sum_q [(1 - \gamma_q^2)^{-1/2} - 1] = 0.156$ in three dimensions for $S = 1/2$. This same result at one-loop level was earlier obtained from a different analysis in terms of the electronic spectral-weight transfer, [13] and is in exact agreement with the SWT result. [20,21]

For arbitrary U , as discussed above Eq. (1), $S \equiv \langle S^z \rangle_{\text{HF}}$ plays the role of the effective spin quantum number. The sublattice magnetization m is therefore obtained from $m = m_{\text{HF}} - \delta m_{\text{SF}}$, where the HF sublattice magnetization is obtained from the self-consistency condition, [18] and the spin-fluctuation correction δm_{SF} at the one-loop level is obtained from Eq. (6) with $S = \langle S^z \rangle_{\text{HF}}$,

$$\delta m_{\text{SF}} = \frac{\langle S^+S^- + S^-S^+ \rangle_{\text{RPA}}}{\langle S^+S^- - S^-S^+ \rangle_{\text{RPA}}} - 1. \quad (7)$$

The U -dependence of the sublattice magnetization $m(U)$ is shown in Fig. 1, showing that it properly interpolates between the weak and strong coupling limits, approaching the SWT result, $m(\infty) = m_{\text{SWT}} = 0.844$ as $U/t \rightarrow \infty$. As expected, the spin-fluctuation correction δm_{SF} increases with interaction strength. We note that the two low- U datapoints are subject to the same finite-size numerical error which affects the transverse spin correlations, as mentioned earlier.

Earlier studies of $m(U)$ have employed self-energy correction ($d = 2$, $m(\infty) \sim 0.7 \neq m_{\text{SWT}}$), [22] the QMC method ($d = 2$), [23] functional-integral schemes ($d = 3$, $m(\infty) = 1.0$), [4] and recently an approximate mapping to an extended-range QHAF with effective U -dependent spin couplings obtained from the *static* transverse spin propagator at the RPA level ($d = 3$, $m(\infty) = m_{\text{SWT}}$). [24] In the last work, use of the static propagator implies that dynamical effects are not fully included, which are in principle important in weak and intermediate coupling regimes when the magnon energy is not negligible compared to the energy gap.

C. Finite temperature

To extend these calculations to finite temperature, we write the diagonal elements $\chi_{ii}^{-+}(\omega)$ and $\chi_{ii}^{+-}(\omega)$ in terms of the RPA-level spectral functions and mode energies as,

$$\chi_{ii}^{-+}(\omega) = \sum_q \left[\frac{-A_q}{\omega - \omega_q} + \frac{B_q}{\omega + \omega_q} \right], \quad (8)$$

and a similar equation for $\chi_{ii}^{+-}(\omega)$ with A_q and B_q interchanged, the symmetry following from the identity $\chi^{-+}(\omega) = \chi^{+-}(-\omega)$. In the strong coupling limit, the spectral functions have the familiar form:

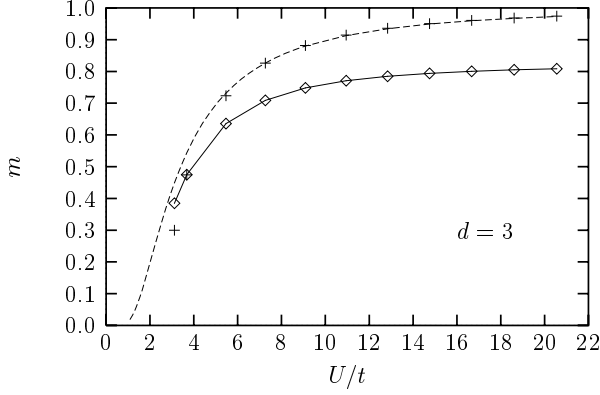


FIG. 1. The sublattice magnetization m vs. U (diamonds), along with the HF results from (i) the self-consistency condition (dashed), and (ii) $\langle 2S^z \rangle_{\text{HF}} = \langle S^+ S^- - S^- S^+ \rangle_{\text{RPA}}$ (plus).

$A_q = [(1 - \gamma_q^2)^{-1/2} - 1]/2$ and $B_q = [(1 - \gamma_q^2)^{-1/2} + 1]/2$. The transverse spin correlations at finite temperature are then obtained conventionally from these propagators by using the Poisson summation formulas which allow replacing the sum over Matsubara frequencies by a contour integral in complex frequency space, and by picking contributions from both poles in the propagators, traversed in the clockwise direction. [25] We obtain,

$$\langle S^- S^+ \rangle = \sum_q \left[\frac{-A_q}{e^{-\beta\omega_q} - 1} + \frac{B_q}{e^{\beta\omega_q} - 1} \right]. \quad (9)$$

Both A_q and B_q are determined from the retarded part of $\chi^{-+}(\omega)$ having positive mode energies by using the spin-sublattice symmetry $\chi_{AA}^{-+}(-\omega) = \chi_{AA}^{+-}(\omega) = \chi_{BB}^{-+}(\omega)$. Thus the spectral functions are obtained from the magnon amplitudes on A and B sublattices using,

$$A_q = \frac{(\phi_q^A)^2}{U^2(d\lambda_q/d\omega)_{\omega_q}}; \quad B_q = \frac{(\phi_q^B)^2}{U^2(d\lambda_q/d\omega)_{\omega_q}}. \quad (10)$$

In analogy with the strong-coupling result discussed above Eq. (2), and in keeping with the renormalization constraints of this RPA theory as discussed above Eq. (1), we now multiplicatively renormalize both the magnon energy ω_q , and the magnon amplitudes A_q, B_q , by multiplying with the momentum-independent ratio $\langle 2S^z \rangle / \langle 2S^z \rangle_{\text{HF}}$. This ensures that the commutation property $[S^+, S^-] = 2S_z$ is satisfied by expectation values in the spin state, as seen below. By separating the zero- and finite-temperature contributions in $\langle S^- S^+ \rangle$ and $\langle S^+ S^- \rangle$ from Eq. (9) and its counterpart, it is seen that $\langle [S^+, S^-] \rangle = \sum_q (B_q - A_q) = \langle 2S_z \rangle_{\text{HF}}$ at all temperatures. This HF result from use of the RPA-level transverse spin correlations is corrected by the above renormalization, and the exact result $\langle 2S_z \rangle$ is obtained instead. Furthermore, as in the strong coupling case, the renormalization of the magnon energy ensures that

the spin stiffness vanishes at the Néel temperature where long-range order vanishes. However, this does not constitute an independent renormalization as, in fact, the two renormalizations of magnon energy and amplitudes are connected. The only renormalization in $\chi^0(\omega)$ (of the ω -term) which affects the magnon amplitudes also modifies the magnon energy in precisely the same manner. [13]

As $T \rightarrow T_N^-$ and $\langle S^z \rangle \rightarrow 0$, we therefore obtain from Eq.(9),

$$\langle S^- S^+ \rangle = \langle S^+ S^- \rangle = T_N \sum_q \left(\frac{\tilde{A}_q + \tilde{B}_q}{\tilde{\omega}_q} \right), \quad (11)$$

where $\tilde{A}_q \equiv A_q / \langle 2S^z \rangle_{\text{HF}}$, $\tilde{B}_q \equiv B_q / \langle 2S^z \rangle_{\text{HF}}$, and $\tilde{\omega}_q \equiv \omega_q / \langle 2S^z \rangle_{\text{HF}}$ are the scaled spectral functions and magnon energies. As for the strong coupling case, T_N is obtained from the isotropy requirement given in Eq. (1), with $\langle \vec{S}^2 \rangle = S(S+1)$ in terms of the effective spin quantum number $S = \langle S_z \rangle_{\text{HF}} = m_{\text{HF}}/2$. With this the Néel temperature is then obtained from

$$T_N = \frac{2}{3} \langle \vec{S}^2 \rangle \left[\sum_q \left(\frac{\tilde{A}_q + \tilde{B}_q}{\tilde{\omega}_q} \right) \right]^{-1}. \quad (12)$$

This result has the proper limiting behavior in both limits. In the weak coupling limit, the magnon energy $\omega_q \approx 2\Delta$, the maximum magnon energy, for almost all q modes. Also $\tilde{A}_q + \tilde{B}_q \approx 1$, so that with $m_{\text{HF}} \approx 0$, we obtain $T_N \sim \Delta$, the proper HF scale. And in the strong coupling limit, $(\tilde{A}_q + \tilde{B}_q)/\tilde{\omega}_q = [3J(1 - \gamma_q^2)]^{-1}$, so that Eq. (3) is obtained, which is in good agreement with the result from high-temperature series expansion, as discussed earlier.

Fig. 2 shows the variation of T_N with U , as obtained from above equation, along with the HF results which is asymptotically approached from below in weak coupling. In strong coupling the result closely approaches the high-temperature series-expansion result $3.83t^2/U$, which is well below the MFT result $6t^2/U$. For weak coupling HF-level finite-temperature effects need to be considered in Eq. (12) when the temperature is not negligible compared to the energy gap, and so it is the effective spin quantum number $S = m_{\text{HF}}/2$ at temperature T_N which is used here. However, the magnon mode amplitudes and energies are obtained at $T = 0$. Determination and use of magnon spectral properties at temperature $T = T_N$ is, of course, possible by iteration, but not very practical. We find that these HF-level finite-temperature corrections become negligible for $U/t > 5$ in the crucial strong correlation limit. On the weak-coupling side of this, the energy gap and therefore the magnon energies ω_q would be reduced somewhat at finite temperature, so that the results for T_N are a slight overestimate for $U/t < 5$.

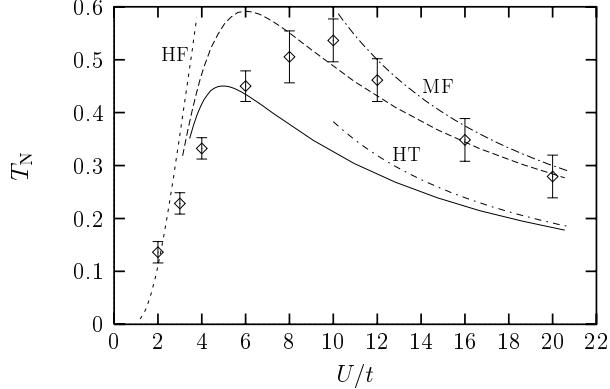


FIG. 2. Néel temperature T_N vs. U/t (solid line), and using the dominant-mode approximation (dashed line). Also shown are the strong-coupling asymptotes MF and HT, from mean-field theory ($T_N^{\text{MF}} = 6t^2/U$) and high-temperature series expansion ($T_N^{\text{HT}} = 3.83t^2/U$) respectively.

D. Dominant-mode approximation

We now consider a dominant-mode approximation which, in the strong coupling limit, becomes equivalent to the dynamical mean-field theory. In the strong-coupling limit, where $\omega_q = dJ\sqrt{1 - \gamma_q^2}$ in d dimensions, the magnon density of states is strongly peaked at the upper band edge at energy dJ , becoming a delta function in the limit $d \rightarrow \infty$. As the highest-energy modes are dominant, in this approximation we only consider these modes in the sum in Eq. (12). As charge fluctuations which have been ignored are absent in the strong coupling limit, and corrections to RPA decrease as $1/d$, this dominant-mode approximation becomes exact in the limit of infinite dimensions. This approximation also becomes good in the weak-coupling limit, where the magnon spectrum is strongly peaked at the gap energy 2Δ , and all fluctuations are weak. Since for the highest-energy modes with $\omega_q = \omega_m$, we have $\hat{A}_q + \hat{B}_q \approx 1$, Eq. (12) simplifies to

$$T_N = \frac{2}{3} \langle \vec{S}^2 \rangle \frac{\omega_m}{2S}, \quad (13)$$

which is also shown in Fig. 2. As $\omega_m = 3J$ in the strong-coupling limit $U/t \rightarrow \infty$, this yields $T_N = 3J/2 = 6t^2/U$, the mean-field result, which is also asymptotically approached in the QMC [7,8] and DMFT [9] calculations. On the other hand, in the limit $U/t \rightarrow 0$, as ω_m approaches 2Δ , the energy gap, we obtain $T_N \sim \Delta$, the proper weak-coupling scale. This analysis indicates that the essential features of the T_N vs. U behavior are contained in ω_m , the energy scale of low-energy spin excitations associated with spontaneous symmetry-breaking of the continuous spin-rotational symmetry. A relationship between T_N and the low-energy scale was also obtained for the infinite-dimensional Bethe lattice. [26]

At finite temperature, the gap parameter Δ is determined from the self-consistency condition, $1/U = \sum_k (1/2E_k) \tanh(\beta E_k/2)$, where $E_k = \sqrt{\Delta^2 + \epsilon_k^2}$ is the AF band energy. In the weak coupling limit, when the temperature is comparable to the interaction strength, the gap parameter, and therefore the maximum magnon energy, are sensitive to temperature. We therefore use $\omega_m(U, T_N)$ in Eq. (13), which is obtained from the magnon spectrum for a gap parameter $\Delta(T_N)$ at temperature T_N . The self-consistent determination of $T_N(U)$ is easily implemented in two steps — (i) obtaining $\omega_m(\Delta)$ and hence $T_N(\Delta)$ as a function of the gap parameter Δ , (ii) then using the self-consistency condition to obtain $U(\Delta, T_N)$. As mentioned earlier, these HF-level finite-temperature corrections become negligible for $U/t > 5$.

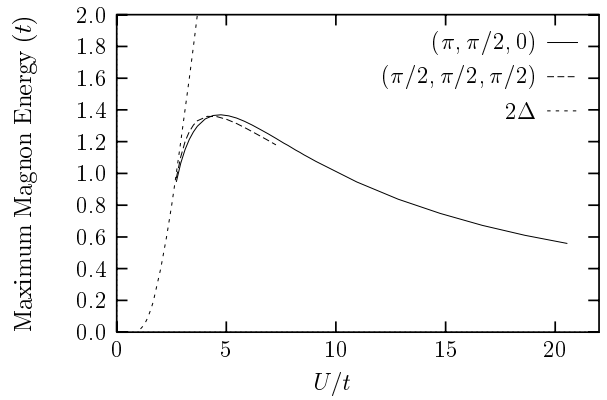


FIG. 3. Magnon energies ω_q vs. U at momenta $(\pi, \pi/2, 0)$ (solid) and $(\pi/2, \pi/2, \pi/2)$ (dashed), together with the Hubbard gap 2Δ (dotted).

The U -dependence of ω_m at $T = 0$ is shown in Fig. 3, showing that it properly interpolates between the two limits. Similar qualitative nature of the U -dependence of the maximum magnon energy was found in two dimensions, [27] and infinite dimensions. [28,26] The complete spectrum of spin excitations was studied earlier for the $d = 2$ case. [27] The band-edge degeneracy at energy $\omega_m = 2J$ in the Heisenberg limit is removed for finite U , and the maximum was found to occur for $q = (\pm\pi, 0)$ and $(0, \pm\pi)$. For $d = 3$ we find that for most of the U/t range the maximum occurs at momenta $q = (\pm\pi, \pm\pi/2, 0)$ etc. where all the $\cos q_\mu$ terms are completely different. For small U (less than about half bandwidth $B/2$) the magnon energy at $(\pi, \pi/2, 0)$ is actually not the maximum, as shown in Fig. 3. However, the difference is marginal, and we have neglected this detail. As the degeneracy of q -points of the type $(\pi, \pi/2, 0)$ is much higher, yielding a correspondingly higher DOS, it is reasonable to use this magnon energy as the relevant energy scale ω_m . This also implies that the structure of the magnon density of states undergoes a crossover (at $U/t \approx 6$), and for small U the peak in magnon density of states changes position from the upper band edge to within the band.

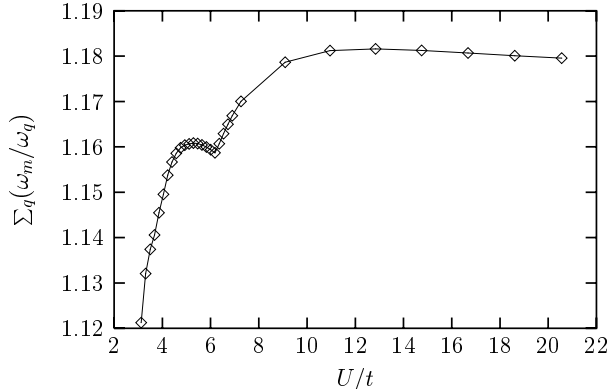


FIG. 4. The mode-averaged ratio $R \equiv \sum_q(\omega_m/\omega_q)$ vs. U , showing the cusp at $U/t \approx 6$, which arises from the red-shift at lower- U of the magnon DOS-peak energy relative to the maximum magnon energy ω_m .

This crossover has been seen in a recent study of the U -dependence of the magnon density of states in $d = 3$. [24]

A convenient way to observe this crossover is through the U -dependence of the mode-averaged ratio $R \equiv \sum_q(\omega_m/\omega_q)$. Here ω_m is the maximum magnon energy (band edge), obtained by sampling through the full spectrum. R approaches 1 in the limit when all magnon modes have energy approaching ω_m . The U -dependence of R is shown in Fig. 4. With decreasing U from the strong-coupling limit, there is at first a marginal increase in R , which then rapidly starts decreasing at $U \approx B$. This decrease in R indicates a reduction in the magnon dispersion, so that relatively more modes have energy closer to the maximum magnon energy ω_m . This trend is, however, sharply cutoff at $U \approx B/2 = 6t$, as clearly seen from the cusp in Fig. 4. The sharp enhancement in R with decreasing U/t is due to the onset of a red-shift of the DOS-peak energy (where the magnon DOS peaks) relative to the band edge, ω_m . Because of this red-shift most magnon modes have energy less than ω_m , yielding an enhanced contribution to R . The rapid decrease in R towards unity with further decrease in U indicates that almost all magnon modes have energy nearly equal to ω_m which, as mentioned earlier, approaches the charge gap 2Δ in weak coupling. The role of the approaching Stoner band in compressing the magnon spectrum has been noted earlier. [27]

In conclusion, this analysis in terms of transverse spin fluctuations at the RPA level provides a good account of the magnetic phase boundary for the three-dimensional, half-filled Hubbard model, particularly in the crucial strong coupling limit. The quantum correction to sublattice magnetization as well as the Néel temperature are obtained in the whole U/t range, and both interpolate

properly between the weak and strong coupling limits. This analysis and the new method to evaluate transverse spin fluctuations should also prove valuable to other related systems such as antiferromagnets with disorder, defects and vacancies, where spin-fluctuation studies can be extended to strong disorder and strong defect/vacancy concentrations.

ACKNOWLEDGMENTS

Helpful conversations with D. Vollhardt and M. Ulmke, and support from the Alexander von Humboldt Foundation through a Research Fellowship are gratefully acknowledged.

-
- * On leave from Department of Physics, Indian Institute of Technology, Kanpur 208016.
- ¹ H. Hasegawa, J. Phys. Soc. Jpn. **49**, 178 (1980).
- ² Y. Kakehashi and J. H. Samson, Phys. Rev. B **33**, 298 (1986).
- ³ Y. Kakehashi and H. Hasegawa, Phys. Rev. B **36**, 4066 (1987); **37**, 7777 (1988).
- ⁴ H. Hasegawa, J. Phys. Condens. Matter. **1**, 9325 (1989).
- ⁵ *Electron Correlation and Magnetism in Narrow-Band Systems*, edited by T. Moriya (Springer-Verlag, Berlin, 1981).
- ⁶ T. Moriya, *Spin Fluctuations in Itinerant Electron Magnetism* (Springer-Verlag, Berlin, 1985).
- ⁷ J. E. Hirsch, Phys. Rev. B **35**, 1851 (1987).
- ⁸ R. T. Scalettar, D. J. Scalapino, R. L. Sugar, and D. Troussaint, Phys. Rev. B **39**, 4711 (1989).
- ⁹ M Jarrell, Phys. Rev. Lett. **69**, 168 (1992); For a review see A. Georges, G. Kotliar, W. Krauth, and M. Rozenberg, Rev. Mod. Phys. **68**, 13 (1996).
- ¹⁰ W. Metzner and D. Vollhardt, Phys. Rev. Lett. **62**, 324 (1989).
- ¹¹ For a recent compilation of earlier results, see reference [12].
- ¹² Y. H. Szczech, M. A. Tusch, and D. E. Logan, Phys. Rev. Lett. **74**, 2804 (1995).
- ¹³ A. Singh, Phys. Rev. B **43**, 3617 (1991).
- ¹⁴ S. Doniach and E. H. Sondheimer, *Green's Functions for Solid State Physicists*, Benjamin/Cummings (1974).
- ¹⁵ R. P. Singh and M. Singh, Phys. Stat. Sol. (b) **169**, 571 (1992).
- ¹⁶ G. S. Rushbrooke, G. A. Baker jr., and P. J. Wood, in *Phase Transitions and Critical Phenomena*, Vol. 3, Chapter 5 (Academic, New York, 1974).
- ¹⁷ See, e.g., R. M. White, *Quantum Theory of Magnetism* (Springer-Verlag, Berlin, 1983).
- ¹⁸ A. Singh and Z. Tešanović, Phys. Rev. B **41**, 614 (1990); Phys. Rev. B **41**, 11 457 (1990).
- ¹⁹ A. Singh and P. Sen, Phys. Rev. B **57**, 10598 (1998).
- ²⁰ P. W. Anderson, Phys. Rev. **86**, 694 (1952).
- ²¹ T. Oguchi, Phys. Rev. **117**, 117 (1960).
- ²² J. R. Schrieffer, X.-G. Wen, and S.-C. Zhang, Phys. Rev. B **39**, 11663 (1989).
- ²³ J. E. Hirsch and S. Tang, Phys. Rev. Lett. **62**, 591 (1989).
- ²⁴ M. A. Tusch, Y. H. Szczech, and D. E. Logan, Phys. Rev. B **53**, 5505 (1996).
- ²⁵ See, e.g., R. J. Schrieffer, *Theory of Superconductivity* (Addison-Wesley, Reading, 1964).
- ²⁶ Y. H. Szczech, M. A. Tusch, and D. E. Logan, J. Phys. Cond. Matt. **9**, 9621 (1997).
- ²⁷ A. Singh, Phys. Rev. B **48**, 6668 (1993).
- ²⁸ D. E. Logan, M. P. Eastwood, and M. A. Tusch, Phys. Rev. Lett. **76**, 4785 (1996).